Published online 5 December 2019

Nucleic Acids Research, 2020, Vol. 48, No. 2 ***847–861***
doi: 10.1093/nar/gkz1152

Cross-subunit catalysis and a new phenomenon of recessive resurrection in *Escherichia coli* RNase E

Nida Ali[1,2] and Jayaraman Gowrishankar[1,*]

[1]Laboratory of Bacterial Genetics, Centre for DNA Fingerprinting and Diagnostics, Hyderabad 500039, India and [2]Graduate Studies, Manipal Academy of Higher Education, Manipal 576104, India

Received October 16, 2019; Revised November 21, 2019; Editorial Decision November 24, 2019; Accepted November 26, 2019

ABSTRACT

RNase E is a 472-kDa homo-tetrameric essential endoribonuclease involved in RNA processing and turnover in *Escherichia coli*. In its N-terminal half (NTH) is the catalytic active site, as also a substrate 5′-sensor pocket that renders enzyme activity maximal on 5′-monophosphorylated RNAs. The protein's non-catalytic C-terminal half (CTH) harbours RNA-binding motifs and serves as scaffold for a multiprotein degradosome complex, but is dispensable for viability. Here, we provide evidence that a full-length hetero-tetramer, composed of a mixture of wild-type and (recessive lethal) active-site mutant subunits, exhibits identical activity *in vivo* as the wild-type homo-tetramer itself ('recessive resurrection'). When all of the cognate polypeptides lacked the CTH, the active-site mutant subunits were dominant negative. A pair of C-terminally truncated polypeptides, which were individually inactive because of additional mutations in their active site and 5′-sensor pocket respectively, exhibited catalytic function in combination, both *in vivo* and *in vitro* (i.e. intragenic or allelic complementation). Our results indicate that adjacent subunits within an oligomer are separately responsible for 5′-sensing and cleavage, and that RNA binding facilitates oligomerization. We propose also that the CTH mediates a rate-determining initial step for enzyme function, which is likely the binding and channelling of substrate for NTH's endonucleolytic action.

INTRODUCTION

In many Gram-negative bacteria (including *Escherichia coli* and *Salmonella enterica*), the endoribonuclease RNase E participates in global mRNA turnover, post-transcriptional maturation of rRNAs and tRNAs, and regulation of stability of small RNAs (sRNAs) and their targets (1–6). It is essential for *E. coli* viability and exists as a homo-tetramer of a 1061-amino acid-long polypeptide that is encoded by the *rne* gene. Expression of *rne* is autoregulated (7–11), since the 5′-untranslated region (5′-UTR) of the *rne* transcript is itself a substrate for the enzyme (12,13).

The properties of RNase E may be discussed in terms of an N-terminal half (NTH) up to residue 529, which bears the catalytic domain, and a non-catalytic C-terminal half (CTH) comprising the remainder. The CTH is intrinsically unstructured and serves as scaffold for assembly of a protein complex called the degradosome (14–19). The latter is comprised of RNase E, polynucleotide phosphorylase (PNPase), RhlB helicase and enolase, and is believed to mediate efficient degradation of structured transcripts. The CTH carries a membrane-targeting sequence (20–23), two RNA-binding domains (18,24), a putative self-oligomerization domain (19), and a region that binds Hfq protein to facilitate the enzyme's interactions with sRNAs (25,26). Nevertheless, the CTH is dispensable for viability.

X-ray crystal structure studies on the NTH of RNase E (both the apoprotein, and its complex with RNA) have established the mechanism of tetramer assembly, which is as a dimer of dimers (27,28). Each NTH protomer is folded into a pair of globular domains, large (residues 1–400) and small (residues 415–529), with an intervening linker containing cysteine residues at positions 404 and 407. The four Cys residues from linker regions of a pair of adjacent subunits co-ordinate a Zn^{2+} atom to form a 'principal' dimer, and the small domains of a principal dimer engage with those of another to constitute the tetramer in a 'twin-scissors' configuration (27,29). The identification of dominant-negative variants of RNase E (30) is consistent with its function as an oligomer.

Residues D303 and D346 are inferred to lie in the active site of RNase E (27). Endonucleolytic activity is highest on RNA with 5′-monophosphate (as compared to 5′-OH, 5′-diphosphate, or 5′-triphosphate) (31–34), and an allosteric '5′-sensor' pocket exists with R169 as a critical residue (27). In the co-crystal structure of enzyme with (non-cleavable) substrate, a single RNA contacts both subunits of the principal dimer, with 5′-end in the sensor pocket of one and the bond for endonucleolytic cleavage in the active site of

*To whom correspondence should be addressed. Tel: +91 40 27216122; Fax: +91 40 27216006; Email: shankar@cdfd.org.in

the other; the possibility of such cross-subunit cleavage in RNase E had been speculated upon earlier (31,35). Nevertheless, no other evidence for a cross-subunit catalytic mechanism is available, and recent models depict 5′-sensing and cleavage to occur within a single subunit (6,36).

An enzyme RppH participates in converting tri- to mono-phosphate at the RNA 5′-end (37,38); 5′-monophosphorylated RNA can also be generated by prior endonucleolytic cleavages. A recent study suggests that RNase E linearly scans RNA from its 5′-end to identify the cleavage site (39).

RNase E can also cleave RNA by an 'internal entry' pathway that is not dependent on 5′-monophosphate, but its mechanism is less clear (40–43); this second pathway possibly requires the CTH (44,45). An R169Q substitution that abolishes 5′-sensing is lethal with CTH truncation but is viable in full-length RNase E (45,46), which has been interpreted as evidence for an additional RNA recognition determinant in the CTH (46). A Δ*rppH* mutant is also viable, but is synthetically lethal with CTH-truncated RNase E (45,47).

The NTH of RNase E is paralogous to RNase G (489 amino acids long), but the latter endonuclease is not essential for viability. It is a homo-dimer with features similar to those in RNase E, including the location of critical active site residues and stimulation by 5′-monophosphate (31–34,48,49).

Although RNase E and its NTH are homo-tetramers, polypeptides with more extensive C-terminal truncations (that are expected to interfere with tetramer assembly and enzyme quaternary structure) still confer viability. (The nomenclature herein is to represent each truncation as NΔ, where N is the residue number at the C-terminal end of the polypeptide; thus the NTH, with residues from 1 to 529, is 529Δ and so on.) Relative to 529Δ, a preparation of 499Δ (with deletion of CTH and part of the small domain) showed more monomers and dimers (50), and also exhibited concentration-dependent catalytic activity (31); a larger truncation 395Δ (that lacks the CTH, the small domain and the residues for Zn^{2+} co-ordination) was predominantly monomeric (48). The catalytic capabilities of both 499Δ and 395Δ were diminished in comparison to that of 529Δ (48,50), but the question that arises is how a protein such as 395Δ could exhibit any activity at all. A 402Δ polypeptide is also catalytically active (51).

In this work, we have examined RNase E variants bearing extended C-terminal truncations in combination with substitutions in the active site or 5′-sensor pocket. We show that intragenic or allelic complementation occurs in RNase E, whereby enzyme activity is restored and strains are rendered viable when pairs of individually inactive mutant proteins are mixed together or co-expressed, consistent with a cross-subunit mechanism of catalysis; such complementation occurs also with the 395Δ variants, where it appears to be mediated by RNA-facilitated oligomerization. We also show that full-length RNase E polypeptides with active-site substitutions that are by themselves lethal can augment the activity *in vivo* of a co-expressed wild-type polypeptide, a novel phenomenon that we refer to as 'recessive resurrection'; accordingly, we propose that the CTH mediates a rate-determining initial step in RNase E function.

MATERIALS AND METHODS

Growth media and bacterial strains

The growth medium was LB (52) unless otherwise indicated, and the growth temperature was 37°C. Supplementation with ampicillin (Amp), chloramphenicol (Cm), kanamycin (Kan), tetracycline (Tet), trimethoprim (Tp) and Xgal were at concentrations described previously (45). Isopropyl β-D-thiogalactoside (IPTG) was added at the indicated concentrations in different experiments.

Genotypes of *E. coli* strains used in the study are listed in Supplementary Table S1, with the following knock-out (Kan^R insertion-deletion) alleles sourced from the collection of Baba *et al.* (53): *lacY*, *pnp*, *recA*, *relA*, *rhlB* and *rng*.

Plasmids and primers

The following plasmids have been described previously (salient features in parentheses): pHYD3004 (54) (Amp^R with ColE1 replicon, for IPTG-mediated T7 promoter-based protein overexpression); pASKA-rne^+ and its corresponding empty vector pCA24N from the ASKA collection (55) (Cm^R with ColE1 replicons, former expresses full-length RNase E with N-terminal His-tag from vector-borne T5-*lac* IPTG-inducible promoter); pWSK29 (56) (Amp^R with pSC101 replicon, which has been used in this study as vector control in the experiments employing derivatives of the related Kan^R pSC101-replicon plasmid pWSK129); pRne-SG1, pRne-SG4, and pRne-SG21 (46) (Kan^R, pWSK129 derivatives expressing, respectively, full-length RNase E, full-length RNase E with R169Q substitution, and RNase E-529Δ with R169Q substitution); pHYD2373 (45) (Kan^R and Cm^R, pWSK129 derivative expressing RNase E-493Δ with R169Q substitution); rne^+ shelter plasmid derivative pHYD1613 and its ancestral vector pMU575 (45) (Tp^R with IncW replicon, with *lacZYA* genes upstream of which, in the latter, there is no promoter and in the former, is the rne^+ gene); and pRC-SpoT (57) (Amp^R with mini-F replicon, carries $spoT^+$ and $lacZ^+$ genes downstream of IPTG-inducible promoter). Plasmids pKD3 (Cm^R Amp^R), pKD13 (Kan^R Amp^R), pKD46 (Amp^R) and pCP20 (Cm^R Amp^R), for use in recombineering experiments and for Flp-mediated site-specific excision of FRT-flanked DNA segments, have been described by Datsenko and Wanner (58).

All other plasmids encoding RNase E variants were constructed in this study, and are described in the *Supplementary Text* and Supplementary Table S2. Oligonucleotide primer sequences are listed in Supplementary Table S3.

Genetic methods

Procedures for P1 transduction (59) and transformation (60) were as described. Recombineering for generation of *rne* truncations on the chromosome and on plasmids was by the methods of either Datsenko and Wanner (58) or Court *et al.* (61), and plasmid pCP20 was used for excision of the FRT-flanked Kan^R or Cm^R determinants, as described (58); the detailed procedures for construction of the different strains and plasmids are described in the *Supplementary Text*. Site-directed mutagenesis on plasmids was performed

by the QuikChange method (Stratagene, USA) with modifications, and the details are provided in the *Supplementary Text*. All constructs from the recombineering and site-directed mutagenesis experiments were verified by DNA sequencing.

Enzyme assays

β-Galactosidase specific activities were determined for chromosomal *rne-lac* and *proU-lac* fusion strains, in cultures grown to mid-exponential phase, by the method of Miller (52) and the values are reported in the units defined therein; mean and standard error values were obtained from at least three experiments. The *lacY* gene in each of the chromosomal *lac* fusion constructs was deleted, so that active transport of externally added IPTG could not occur into the cells. When *rne-lac* expression was measured in strains also carrying the *rne*$^+$ shelter plasmid pHYD1613 or its derivatives, the *lacZ* gene on the plasmid was disrupted with the *lacZ4526*::Tn*10*dTet insertion that was sourced from strain GJ2278 (62).

RNase E assays were performed essentially as described (41), with a 13-mer RNA substrate BR13 (5′-GGGACAGUAUUUG-3′) which was monophosphorylated and fluorescein-conjugated at its 5′- and 3′-ends, respectively (obtained from Sigma Chemicals, USA); cleavage by RNase E leads to the release of a pentanucleotide product with the fluorescein tag. The reaction mixture was similar to that of Caruthers *et al.* (48), with enzyme activity being determined at 30°C in a 20-μl volume [containing 20 mM Tris–Cl (pH 8), 10 mM $MgCl_2$, 10 mM NaCl, 0.1 mM dithiothreitol and 20 U of RNaseOUT recombinant ribonuclease inhibitor (Thermo Fisher Scientific, USA)] after addition of 1 pmol of the protein preparation(s) and 2 pmol of substrate; at different time points, 6 μl aliquots were removed and the reactions were terminated by addition to each of an equal volume of loading dye [95% formamide, 18 mM EDTA and 0.025% each of sodium dodecyl sulphate (SDS), xylene cyanol, and bromophenol blue]. The samples were denatured at 85°C for 3 min and then subjected to electrophoresis on an 8 M urea–15% polyacrylamide gel (60). Fluorescent bands in the gel were detected with a Fujifilm FLA9000 scanner, using 473 nm laser for excitation and LPB (>520 nm) as emission filter.

Reverse transcriptase-quantitative PCR (RT-qPCR)

RT-qPCR experiments were performed and are reported below in conformity with the MIQE guidelines (63). The detailed methods are described in the *Supplementary Text*, and data normalizations and analyses were performed essentially as described (64).

Other methods

Growth rates of cultures were determined on a Varioskan FLASH microplate reader (Thermo Fisher Scientific). The protocols of Sambrook and Russell (60) were followed for DNA manipulations and analysis, and transformants following plasmid ligations were recovered in strain DH5α. DNA sequencing was performed in the institute's central facility. His-tagged truncated RNase E variants were purified following their overexpression by IPTG induction, either from ASKA-*rne*-derived plasmids (55) or in strain BL21(DE3) (65), as more fully described in the *Supplementary Text*; high-salt conditions were employed during protein purification (66), in order to avoid contamination by host-encoded RNase E in the preparations. The proteins were stored at −80°C in the buffer described by Shin *et al.* (67), with 20% glycerol. The procedures followed for size-exclusion chromatography and RNase E immunoblotting are also described in the *Supplementary Text*.

RESULTS

Description of RNase E variants and the assays for their contributions to viability and *in vivo* activity

The C-terminal truncations of RNase E used were (description of regions deleted in parentheses, see Figure 1A): 529Δ (CTH); 493Δ (CTH and part of small domain); 438Δ (CTH and major portion of small domain); 418Δ (CTH and entire small domain) and 395Δ (CTH, small domain, and linker residues for Zn^{2+} co-ordination). The substitutions, generated in full-length RNase E or the truncation variants, were (affected region in parentheses): D303A (active site); D346A (active site); and R169Q (5′-sensor pocket). The *rne* gene location for this repertoire of variants included: (i) native chromosomal locus; (ii) plasmid pRne-SG1 (pSC101 replicon, low-copy-number); (iii) plasmid pHYD1613 (IncW replicon, single-copy-number); or (iv) plasmid pASKA-*rne*$^+$ (ColE1 replicon, high-copy-number, gene expression inducible with IPTG).

Viability of any RNase E variant was tested by expressing it in a strain that was Δ*lac* and Δ*rne* on the chromosome and carrying the shelter plasmid pHYD1613. The latter is *rne*$^+$ *lacZ*$^+$ and lacks a stringent partitioning mechanism, so that ∼3–20% of cells in a culture (in absence of selection) are plasmid-free. Such plasmid-free cells grow as white colonies on Xgal-supplemented plates (and can be successfully subcultured) if the expressed RNase E variant confers viability, whereas if it is lethal the proportion of white colonies to total is <0.2%. We have employed the analogous 'blue-white' screening approach earlier in studies of other essential genes (68–70).

The assay for *in vivo* RNase E activity relies on the fact that *rne* expression is autoregulated. Thus, expression of a chromosomally integrated P_{rne}-*lac* (hereinafter referred to as *rne-lac*) is an inverse measure of intracellular RNase E activity (8,10,11).

Viability of RNase E truncations, and lethality associated with active-site and 5′-sensor mutations

Using the blue-white screening assays, we confirmed that three RNase E variants in which the CTH and contiguous regions of the NTH were deleted (493Δ, 438Δ, and 418Δ) conferred viability when expressed from the native chromosomal locus (Figure 1B, panels iii–v), as too did the wild-type polypeptide (Figure 1B, panel ii); the Δ*rne* mutation was lethal (Figure 1B, panel i). A fourth truncation, 395Δ, was lethal in the chromosomal location (Figure 1B, panel vi).

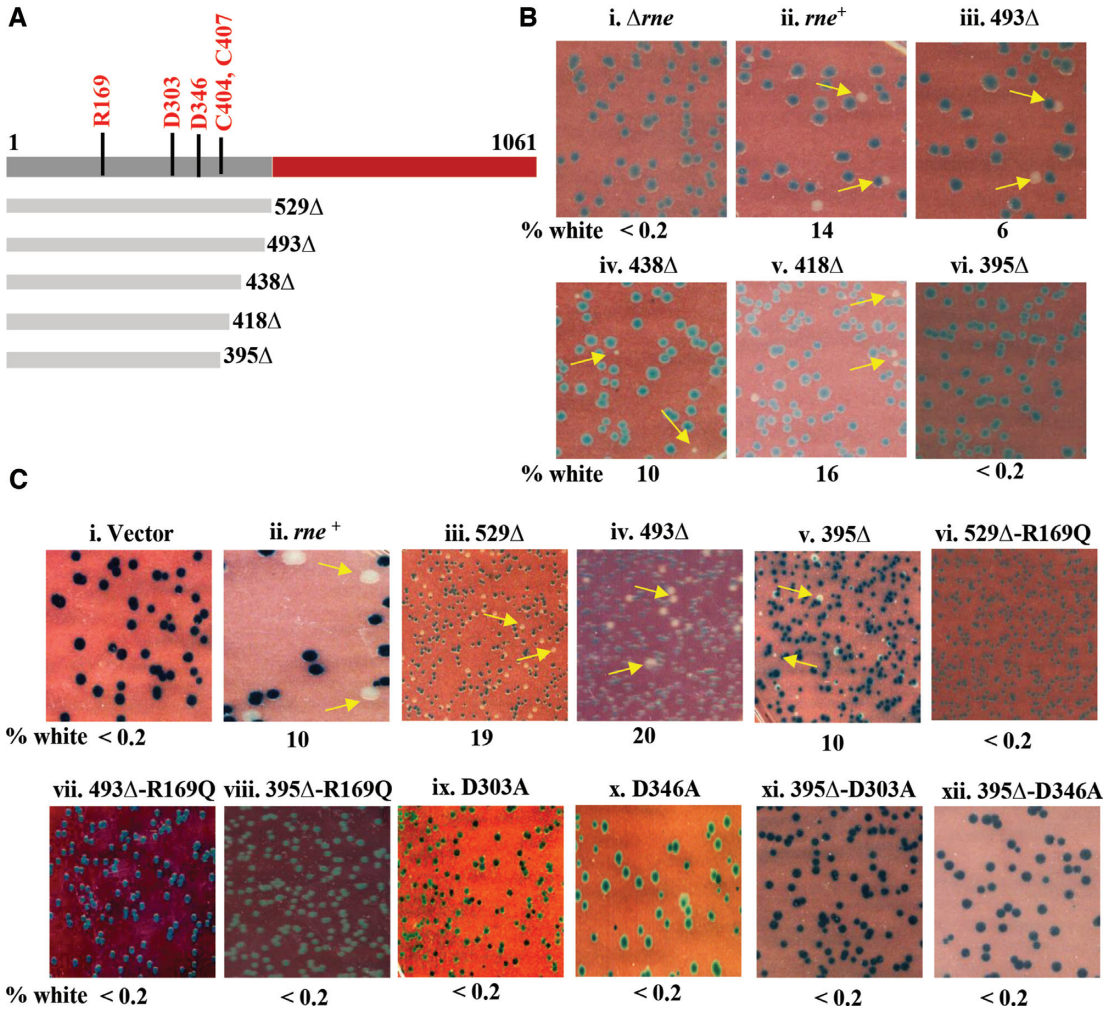

Figure 1. Determination of viability conferred by RNase E variants. (**A**) Linear representation of the 1061-amino acid-long RNase E polypeptide, and of its C-terminal truncation variants after alignment to the former. Depicted are the NTH (dark grey) and CTH (red) regions of RNase E, and the positions of the residues R169 (5′-sensor), D303 and D346 (active site), and C404 and C407 (for coordination with Zn^{2+}). (**B**) Blue-white screening assays with *rne*$^+$ shelter plasmid pHYD1613 and different chromosomal *rne* constructs (as indicated on top of each panel). Representative images are shown, and the numbers beneath each of the panels indicate the percentage of white colonies to the total, that is, viable even in absence of *rne*$^+$ shelter plasmid (minimum of 500 colonies counted). Examples of white colonies are marked by the yellow arrows. Strains employed for the different panels were pHYD1613 derivatives of: i, GJ15079; ii, GJ1499; iii, GJ15078; iv, GJ15020; v, GJ15019 and vi, GJ15018. (**C**) Blue-white screening assays (as in panel B) to determine viability conferred by RNase E variants encoded by ASKA- or pWSK129-plasmid derivatives in Δ*rne* strain GJ12087. Plasmids used in the different panels were (variant encoded indicated on top of each): i, pCA24N; ii, pASKA-*rne*$^+$; iii, pHYD5194; iv, pHYD5183; v, pHYD5166; vi, pRne-SG21; vii, pHYD2379; viii, pHYD5168; ix, pHYD5152; x, pHYD5151; xi, pHYD5182; and xii, pHYD5181. For panels i-iv and ix–x, the plates were supplemented with 10 μM IPTG. For panels v and xi–xii, the plates were supplemented with 100 μM IPTG and the shelter plasmid used was pHYD5193 which is a Δ*lac Y* derivative of pHYD1613 (so that IPTG accumulation to toxic levels does not occur in the blue colonies).

Cohen and coworkers (48) had shown that overexpression of 395Δ confers viability. We too found that 395Δ confers viability when expressed from an IPTG-inducible promoter on a multicopy plasmid, but only so with higher IPTG supplementation (100 μM) than that required for constructs expressing the full-length polypeptide and its 529Δ or 493Δ derivatives (10 μM) (Figure 1C, compare panel v with panels ii–iv).

Concerning the substitution variants, earlier work had shown that 5′-sensor substitution R169Q is lethal in combination with CTH deletion but is viable in full-length RNase E (45–47); in this study as well, R169Q was lethal with the 529Δ, 493Δ and 395Δ truncations (Figure 1C, panels vi–viii). Lethality of active site substitutions D303A or D346A had also been demonstrated earlier (34), and we confirmed that they are inviable in both full-length RNase E (Figure 1C, panels ix–x) and 395Δ (Figure 1C, panels xi–xii).

Reduction in specific activity and increase in dominant negativity with progressive truncations in RNase E

Through *rne-lac* assays, we showed that there is progressive reduction in enzyme specific activity with increasing lengths of C-terminal truncation of RNase E; these experiments were done in strains in which the truncation variants were the only RNase E-derived polypeptides being expressed (from P_{rne} on single-copy-number plasmid replicon). The decrease was around 3-, 7- and 10-fold with trun-

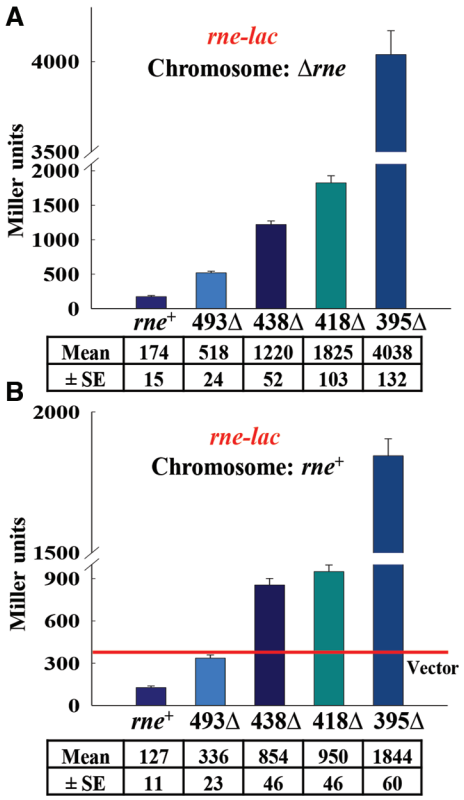

Figure 2. β-Galactosidase specific activity (Miller units ± SE) in *rne-lac* strains (GJ15071 and GJ15068 respectively) bearing Δ*rne* (**A**) or *rne*$^+$ (**B**) on the chromosome, carrying single-copy-number plasmid derivatives encoding the indicated RNase E variants. Plasmids in the different derivatives were: vector, pMU575; *rne*$^+$, pHYD5159; 493Δ, pHYD5158; 438Δ, pHYD5157; 418Δ, pHYD5156 and 395Δ, pHYD5155. The value for vector in the *rne*$^+$ strain (390 ± 22) is marked by the red horizontal line in panel B.

cations beyond residues 493, 438 and 418, respectively (Figure 2A). In another experiment performed with multicopy ASKA plasmid derivatives, we inferred that specific activities of 529Δ and 493Δ (following induction with 25 μM IPTG) are similar to one another and ∼4-fold less than that of wild-type RNase E (Supplementary Figure S1A).

The 395Δ construct, which was lethal at its chromosomal locus, could confer viability when on the single-copy-number plasmid. Since the *rne* gene on the chromosome is positioned near the replication terminus region, we expect the copy number for plasmid-borne *rne* to be around twice that on the chromosome during exponential growth in LB medium (71). The specific activity of 395Δ was at least 20-fold less than that of the wild-type enzyme (Figure 2A), with autoregulation then serving to buffer this reduction.

By performing *rne-lac* assays in strains that were *rne*$^+$ on the chromosome, the dominant-negativity of the different plasmid-encoded RNase E variants was determined. Each of the latter was expressed from P_{rne} on the single-copy-number plasmid, with full-length RNase E similarly expressed serving as control (Figure 2B, the value for plasmid vector is shown by the red horizontal line).

With *rne*$^+$ on the plasmid, there was an ∼3-fold reduction in *rne-lac* expression compared to the value for vector (which is consistent with the estimated plasmid gene dosage of two per chromosomal copy of *rne*$^+$, as mentioned above). With *rne*-493Δ on the plasmid, *rne-lac* activity was similar to that with vector alone, which we believe may reflect the opposing influences of additivity of enzyme activity on the one hand and dominant negativity of 493Δ on the other. With the more extensive truncations (438Δ, 418Δ and 395Δ), their dominant negativity was unambiguous since *rne-lac* expression was significantly elevated over that in the vector-bearing strain; these data are consistent with earlier findings that C-terminal truncations of RNase E are dominant negative (30).

We also examined the effects of ASKA-encoded 529Δ, 493Δ and 395Δ (induced with different IPTG concentrations) in the *rne*$^+$ *rne-lac* strain (Supplementary Figure S1B). One can infer that all three variants are associated with lower RNase E activity than that obtained with ASKA-encoded *rne*$^+$. Furthermore, *rne-lac* expression was moderately higher in the 493Δ-bearing derivative than in that with 529Δ at all IPTG concentrations, which was statistically significant ($P < 0.03$, paired t-test); the implication is that 493Δ is more dominant negative than 529Δ, which is consistent with the finding of Baek *et al.* (50) that 499Δ is less catalytically proficient than 529Δ (on sRNA-paired targets). As expected, 395Δ exhibited pronounced dominant negativity, especially with 100 μM IPTG.

Our results therefore establish a correlation between increasing lengths of RNase E truncation on the one hand and progressive reductions in enzyme specific activity and enhancements in dominant negativity on the other. The fact that 395Δ is dominant negative indicates that it is proficient for oligomerization *in vivo*.

Restoration of RNase E activity *in vivo* with pairs of individually inactive polypeptides

Luisi and coworkers had proposed that adjacent subunits in the RNase E tetramer are separately responsible for RNA 5′-end sensing and cleavage (27,28), although more recent models from their group (6,36) suggest that both occur within a single subunit. We reasoned that if the former model of cross-subunit catalysis is correct, then intragenic or allelic complementation may be demonstrable; that is, a pair of individually inactive polypeptides with substitutions in the active site and 5′-sensor pocket, respectively, would in combination be proficient for RNase E activity.

Accordingly, we tested derivatives in which polypeptides with active site substitutions D303A or D346A on the one hand and a 529Δ or 493Δ variant with R169Q substitution on the other were co-expressed. As noted above, each of these by itself is lethal. The 'blue-white' screening assays depicted in Figure 3 (panels i-iii) indicate that co-expression of the polypeptide pairs restored viability. There was no viability when the R169Q and D303A/D346A substitutions were present on the same polypeptide (Figure 3, panels iv–v).

Rescue through such combined expression was observed also in strains in which the D303A- or D346A-bearing polypeptides (on either full-length RNase E or 493Δ) were down-regulated because of a 15-bp deletion in the promoter region of the ASKA plasmid vector (Supplementary Fig-

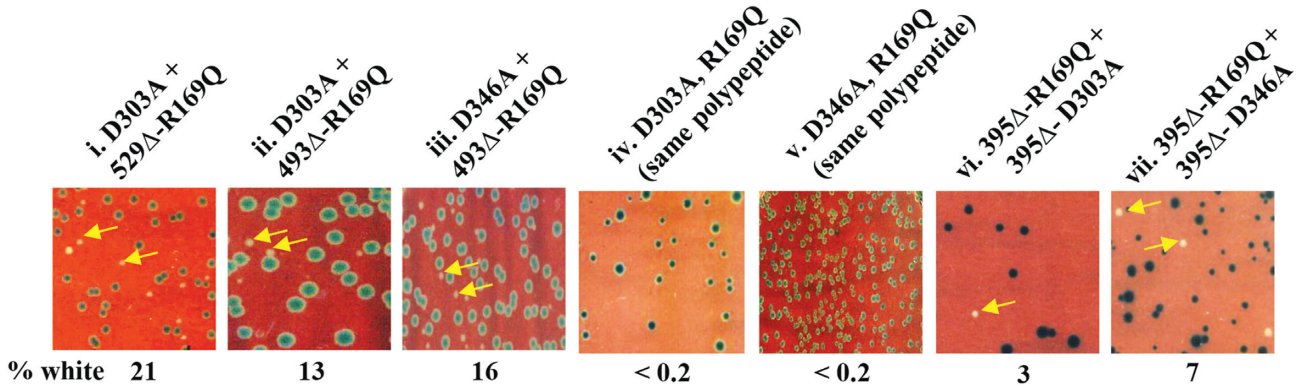

Figure 3. Restoration of viability upon co-expression of pairs of lethal *rne* alleles (intragenic complementation). Blue-white screening assays were performed with *rne*$^{+}$ shelter plasmid in chromosomal Δ*rne* strains GJ12087 (panels i–v) or GJ16199 (panels vi–vii), in which pairs of RNase E variants were co-expressed (or just one polypeptide with two substitutions as control) as indicated on the top of each panel. Representative images are shown, and the percentage of white colonies to total for each panel is indicated as explained in the legend to Figure 1B. Plasmids employed for the different panels were: i, pHYD5152 and pRne-SG21; ii, pHYD5152 and pHYD2379; iii, pHYD5151 and pHYD2379; iv, pHYD5165; v, pHYD5164; vi, pHYD5182 and pHYD5168 and vii, pHYD5181 and pHYD5168. For panels i–v, the shelter plasmid was pHYD1613 and plates were supplemented with 10 μM IPTG; for panels vi–vii, the shelter plasmid was the Δ*lacY* derivative pHYD5193 (for reasons explained in legend to Figure 1C) and IPTG supplementation was at 100 μM.

ure S2, panels i–iv). Intragenic complementation with the down-regulated promoter was successful even in strains that were ppGpp^{0} (that is, Δ*relA* Δ*spoT*) and lacking RNase G (Supplementary Figure S2, panels v–vi); both these perturbations increase the stringency of RNase E essentiality in *E. coli* (47).

Co-expression of a pair of individually inactive 395Δ variants, one with R169Q and the other with either D303A or D346A, was also associated with rescue of Δ*rne* lethality (Figure 3, panels vi–vii). These data provide support for two conclusions, that RNase E can act through a cross-subunit mechanism of catalysis, and that 395Δ can oligomerize *in vivo*.

In vitro confirmation of intragenic complementation in RNase E

To test whether intragenic complementation could be reproduced *in vitro*, the cognate (His-tagged) RNase E polypeptides were overexpressed and purified (Figure 4A). The enzyme assay was based on that described previously (41), in which the substrate is a 13-mer fragment of the ColE1 plasmid-encoded RNA-I (5′-monophosphorylated and fluorescein-labelled at its 3′-end); it is cleaved by RNase E to yield a fluorescent pentanucleotide product that is detected following electrophoresis on denaturing polyacrylamide gels.

With both RNase E-493Δ and −395Δ, there was a time-dependent increase in product formation (Figure 4B, lanes 2–4 and 5–7, respectively). No product formation was observed with 395Δ variants bearing either D346A or R169Q substitutions (Figure 4B, lanes 8–10 and 11–13, respectively); in combination, however, the two polypeptides exhibited substrate cleavage activity (Figure 4B, lanes 14–16). Similar data were obtained in an independent experiment (Supplementary Figure S3), which showed additionally that 395Δ-D303A is inactive but catalyzes time-dependent product accumulation in combination with 395Δ-R169Q. Densitometric analysis revealed that after 15 min, product yields were around 20-fold higher in presence of 493Δ, 395Δ, 395Δ-D346A + 395Δ-R169Q, or 395Δ-D303A + 395Δ-R169Q polypeptides compared to that upon addition of no or any single inactive polypeptide, and that ∼25% of RNA was cleaved in these reactions within this period.

Change in oligomerization status of RNase E-395Δ and -493Δ in presence of RNA

The crystal structures of RNase E NTH (529Δ) reveal it to be a homo-tetramer both in presence or absence of RNA (27,28). Experiments of size-exclusion chromatography have shown that (i) 529Δ is a tetramer (50,72,73); (ii) 499Δ is populated with less tetramers and an increase of dimers and monomers, relative to 529Δ (50) and (iii) 395Δ is a monomer (48).

On the other hand, our findings on dominant negativity and intragenic complementation strongly suggested that 395Δ can assemble as hetero-oligomers. To reconcile these conflicting conclusions, we reasoned that oligomerization of RNase E variants with extended C-terminal truncations (such as 395Δ or 493Δ) may be influenced by their binding to RNA; accordingly, we undertook size-exclusion chromatography experiments with these proteins in presence and absence of RNA. The latter was a 5′-monophosphorylated 13-mer (similar to that in RNA-I) but bearing 2′-methoxy groups so that it could bind the protein but not be cleaved, and has been described earlier (27).

The data from the chromatography experiments are presented in Figure 5. Since the column's void volume was 4.7 ml, A_{280} peaks at elution volumes <1 ml (that is, in the column flow-through) have not been taken into consideration in the analysis below. In absence of RNA, the 395Δ polypeptide eluted as a single sharp peak at 9.4 ml in presence of 100 mM NaCl (Figure 5B, black), and predominantly between 9 and 9.4 ml (as two overlapping peaks) with 10 mM NaCl (Figure 5B, red); the size marker proteins bovine serum albumin (66 kDa) and carbonic anhydrase (29 kDa) eluted at 6.0 ml and 7.1 ml respectively (Figure

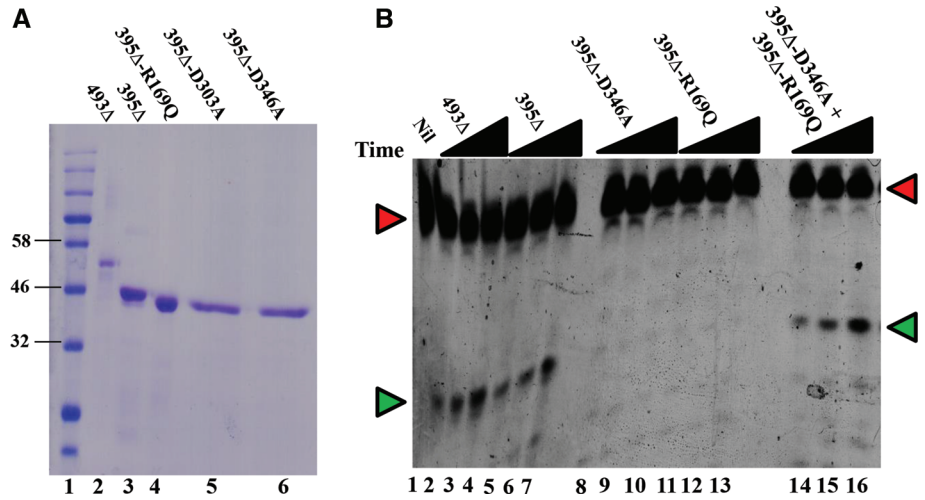

Figure 4. *In vitro* reconstitution of intragenic complementation in RNase E. (**A**) Visualization by Coomassie blue staining of purified preparations of RNase E variants following electrophoresis on SDS–10% polyacrylamide gel. Lane 1, molecular-weight standards; values (in kDa) for some of the bands on this lane are indicated. (**B**) Determination of catalytic activity for RNase E variants singly and in combination. The proteins tested are indicated on top, and each wedge represents increasing reaction times (5, 10 and 15 min) from left to right. For lanes 14 to 16, the polypeptides were pre-mixed immediately before their addition to the reaction mixture. Positions of migration of 13-mer RNA substrate and 5-mer product, both fluorescein-tagged, are marked by red and green arrowheads, respectively.

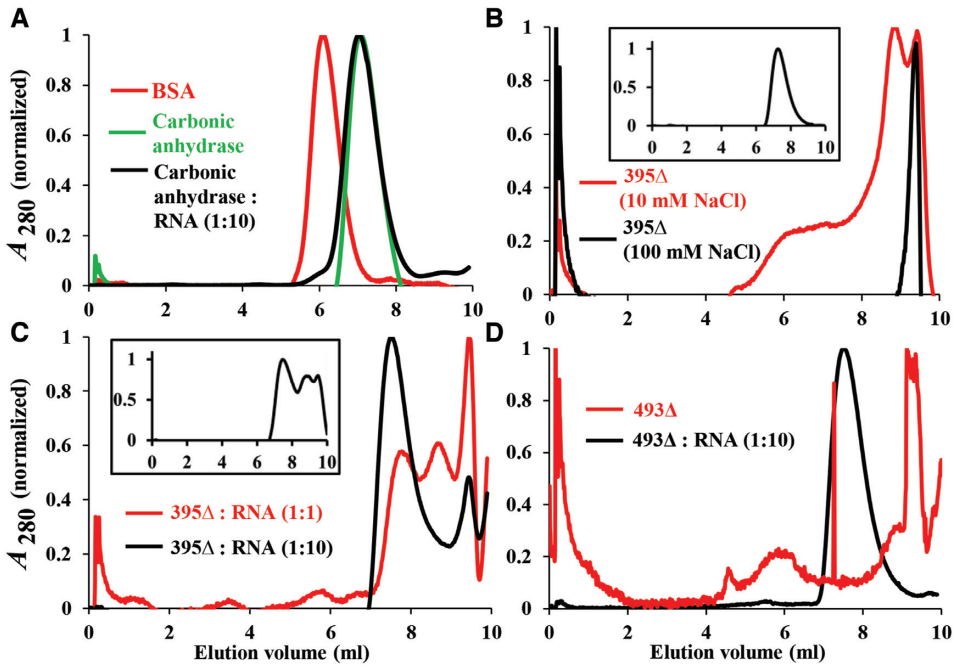

Figure 5. Size-exclusion chromatography of control proteins and of RNase E-395Δ and -493Δ variants in absence or presence of non-cleavable RNA. A_{280} elution profiles are shown, after normalization of each profile to its peak value (taken as 1). Description of input materials (and buffer condition changes, if any) are given in the keys to individual panels. Insets to panels **B** and **C** depict normalized A_{280} elution profiles upon re-chromatography of the pooled eluate fractions from, respectively: 8.3 ml to 9.8 ml of red trace in panel B, performed after addition of 10-fold excess of RNA; and 6.8 to 8.3 ml of black trace in panel C. BSA, bovine serum albumin.

5A, red and green, respectively). We surmise that RNaseE-395Δ elutes as a monomer [in agreement with Caruthers *et al.* (48)], which apparently migrates more slowly than expected for its size. The more complex elution pattern for 395Δ in 10 mM NaCl could possibly be related to formation of protein aggregates that dissociate during the column run.

We repeated the experiments after adding the 13-mer non-cleavable RNA to the 395Δ preparation at 10:1 and 1:1 molar ratios (in buffer with 10 mM NaCl). At the 10:1 ratio, a majority of the 395Δ polypeptide eluted earlier from the column as a peak at around 7.6 ml, with a small residual at 9.2 ml (Figure 5C, black). With the lower molar ratio of added RNA, the elution trace was intermedi-

ate to those without RNA and with RNA at 10:1 (Figure 5C, red). We interpret these findings as evidence for RNA-facilitated dimerization of the 395Δ polypeptide. In a control experiment, addition of RNA to carbonic anhydrase (at 10:1 ratio) had no effect on the latter's elution (Figure 5A, black).

Two lines of evidence were obtained to show that the slower elution profile for 395Δ during chromatography in absence of RNA was not because of degradation of the polypeptide. First, when fractions centred around the overlapping peaks between 9 and 9.4 ml (for red trace of Figure 5B) were pooled and electrophoresed on an SDS-polyacrylamide gel, the protein's mobility remained identical to that of 395Δ (Supplementary Figure S4, compare lanes 2 and 3). Second, when these pooled fractions were re-chromatographed after addition of RNA (in 10-fold excess), the protein now eluted faster, with peak at the 7.6-ml position surmised for the dimer (Figure 5B, inset).

We also performed the reverse experiment of pooling fractions encompassing the faster-eluting peak in presence of RNA (that is, centred around 7.6 ml in black trace of Figure 5C) and re-chromatographing the protein in them. The elution pattern (Figure 5C, inset) was now shifted towards that for 395Δ with 1:1 RNA:protein, with the monomer elution peak at around 9.4 ml becoming more prominent than that at the 10:1 ratio. These results are consistent with reversible RNA-dependent inter-conversion between monomer and dimer species for the 395Δ protein, and furthermore serve to confirm that the protein remained intact during the chromatographic procedures in presence and absence of RNA.

With the 493Δ preparation as well, a prominent elution peak at 9.2 ml in absence of RNA was advanced to 7.5 ml in presence of 10-fold molar excess of the RNA substrate (Figure 5D, red and black, respectively), suggestive of RNA-facilitated monomer-to-dimer conversion; once again as with 395Δ, the 493Δ polypeptide in absence of RNA exhibited some complexity in its elution at 10 mM NaCl. Overall, however, our results do suggest that oligomer assembly in both RNase E-395Δ and −493Δ may be stabilized by a cross-subunit mode of RNA binding to the protomers, which would then be accompanied by the conformational changes observed in structural studies upon RNA binding to RNase E (27,28,74).

Active site and 5′-sensor mutations confer dominant negativity when they are present on RNase E polypeptides that are ΔCTH

Mutations disrupting the active site in an oligomeric enzyme are expected to be dominant negative, on the rationale that the mutant polypeptides will act as subunit poisons within the mixed oligomers (75,76). RNase E is unusual in that it is only its truncation mutants that are dominant negative [(30), confirmed also in this study], whereas inactive missense mutants in the full-length polypeptide are not so (30).

We therefore asked whether the exhibition of dominant negativity by lethal active-site or 5′-sensor RNase E substitutions might require the co-expressed 'killer' and target polypeptides also to be CTH-truncated, and accordingly undertook experiments in *rne-lac* derivatives in which the chromosomal *rne* gene was truncated as to encode RNase E-493Δ. For testing the 5′-sensor substitution (R169Q), we used plasmids expressing RNase E-493Δ with or without R169Q from the native promoter (along with the plasmid vector control); the results indicate that the 493Δ-R169Q construct is associated with higher *rne-lac* expression than even that obtained with the vector (Figure 6A). Similarly, the active-site substitution (D346A) was tested with plasmids expressing either 493Δ or 493Δ-D346A from an IPTG-inducible promoter; it was only for the 493Δ-D346A construct that an IPTG-dependent increase in *rne-lac* expression was observed, indicative of dominant negativity (Figure 6B). Thus, by employing a CTH-truncated protein as sole source of functional RNase E, we could show that co-expressed polypeptides with active-site or 5′-sensor substitutions are dominant negative.

We also found that the hitherto known dominant negativity of CTH-truncated polypeptides over full-length RNase E (30, and Figure 2B) is accentuated when the former also carried active site or 5′-sensor substitutions; these experiments were performed in an *rne-lac* derivative which was chromosomally *rne*$^+$, and expression of the CTH-truncated variants without or with the active site/5′-sensor substitutions (from either the native promoter or IPTG-inducible promoter) was achieved from plasmids; the cognate plasmid vectors served as controls. Thus, expression from the native promoter of 493Δ-R169Q was associated with higher *rne-lac* expression compared to 493Δ or the vector (Supplementary Figure S5A); and 493Δ-D346A expressed from an IPTG-inducible promoter imposed dose-dependent increase in *rne-lac* expression that was much higher than that for 493Δ or the vector (Supplementary Figure S5B). An R169Q substitution on 529Δ also conferred dominant negativity in the *rne*$^+$ strain to similar extent as did 493Δ-R169Q, with *rne-lac* values elevated above that in the vector-bearing derivative (Supplementary Figure S5A). These data therefore support the notion that the substitutions in the CTH-truncated polypeptides are more dominant negative over full-length RNase E than are the CTH truncations themselves.

Similarly in the chromosomally *rne*$^+$ *rne-lac* strain, we expressed from the ASKA derivatives (at progressively higher levels) the 395Δ polypeptide as such, or with the active site substitutions D303A or D346A. The active site substitution variants in 395Δ were more strongly dominant negative than 395Δ itself, as evidenced from the *rne-lac* expression values at 50 μM IPTG (Supplementary Figure S5C). The growth rates of derivatives expressing 395Δ without or with D303A or D346A were similar to one another and to the vector (pCA24N)-bearing strain, with at best a marginal decrease between 0 and 50 μM IPTG (Supplementary Table S4); however, at 100 μM IPTG, the 395Δ derivative itself continued to be viable but the strains expressing 395Δ with the active site substitutions were sick and overpopulated by suppressor mutants so that their *rne-lac* expression values could not be ascertained.

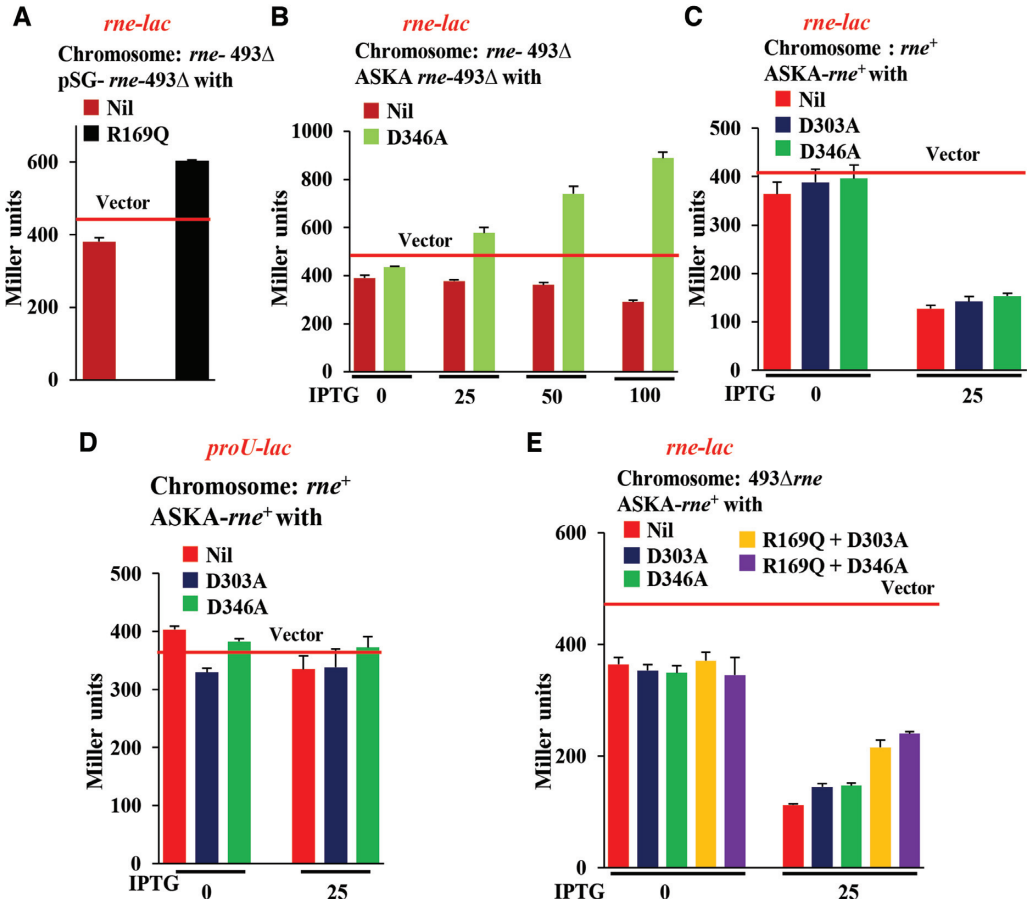

Figure 6. β-Galactosidase specific activity (Miller units) in *rne-lac* strains bearing *rne*-493Δ (**A**, **B** and **E**) or *rne*$^+$ (**C**) on the chromosome, and in the chromosomal *rne*$^+$ *proU-lac* strain (**D**), upon expression of the indicated RNase E substitution variants from different plasmids. Red horizontal line in each panel represents the value for the corresponding vector derivative (pWSK29 for panel A, and pCA24N for panels B–E). The key to each panel describes the *lac* fusion, chromosomal *rne* genotype, and salient features of the plasmids used. IPTG concentrations used (in μM) for culture supplementation in panels B-E are indicated. The growth medium for experiments with *proU-lac* fusion strains (panel D) was LB supplemented with 0.1 M NaCl. Strains employed were: (A) GJ15070; (B and E) GJ15075; (C) GJ15074 and (D) GJ15077. Plasmids in the different derivatives were as follows. (A) Nil, pHYD5101; and R169Q, pHYD2379; (B) 493Δ, pHYD5183; and 493Δ-D346A, pHYD5180; (C and D) Nil, pASKA-*rne*$^+$; D303A, pHYD5152 and D346A, pHYD5151 and (E) Nil, pASKA-*rne*$^+$; D303A, pHYD5152; D346A, pHYD5151; R169Q + D303A, pHYD5165 and R169Q + D346A, pHYD5164.

Evidence for equivalent *in vivo* activities for a full-length RNase E tetramer with one or four active polypeptides: recessive resurrection

The results above showed that active site and 5′-sensor substitutions in CTH-truncated RNase E mediate subunit poisoning when hetero-oligomerized with functional RNase E polypeptides (full-length or CTH-truncated). We next examined how these substitutions on a full-length polypeptide would affect enzyme activity in hetero-oligomers. We accordingly measured the effects on *rne-lac* expression, in a chromosomally *rne*$^+$ strain, of increased production of full-length RNase E polypeptides without or with the concerned substitutions (achieved by 25 μM IPTG induction from ASKA plasmid constructs). Δ*recA* derivatives were used to ensure that the mutations could not revert to wild-type through homologous recombination.

With the ASKA-*rne*$^+$ plasmid, *rne-lac* expression was reduced upon IPTG supplementation, which is as expected in light of RNase E autoregulation (Figure 6C, red bars). Most unexpectedly, however, identical results were obtained also with the ASKA plasmid derivatives encoding the active site substitutions D303A or D346A on full-length RNase E (Figure 6C, blue and green bars, respectively); we confirmed by PCR and DNA sequencing that the two cultures indeed carried the cognate mutations (Supplementary Figure S6A). β-Galactosidase expression from a control *lac* fusion [*proU-lac*, which ordinarily is osmotically regulated (59)] was unaffected by overproduction of wild-type or the mutant RNase E polypeptides (Figure 6D), indicating that the observed effects were specific to *rne-lac*.

There is evidence to suggest that, at slow growth rates, *rne-lac* expression may be lower than that predicted from a simple model of its inverse proportionality with intracellular RNase E activity (11); we therefore asked whether the reduction in *rne-lac* expression in strains expressing the polypeptides with active site substitutions might be an artefact of decreased growth rate. However, there were no differences in growth rates between the derivatives with ASKA plasmid vector (pCA24N) on the one hand and constructs expressing full-length RNase E without or with D303A or D346A on the other, at 0 or 25 μM IPTG (Supplementary

Table S4), which was consistent also with the qualitative assessments on agar plates.

Therefore, these observations with overexpression of the mutant genes indicated the opposite of a dominant negative effect and were counterintuitive, since they imply that *in vivo* RNase E activity is enhanced upon co-expression of enzymatically dead polypeptides. The following calculation provides an estimate of the magnitude of such an effect. With wild-type *rne*$^+$ on the ASKA plasmid and 25 μM IPTG, there is an approximate 3-fold decrease in chromosomal *rne-lac* expression (relative to that in the vector-bearing strain, Figure 6C); this would suggest a 2:1 ratio of production in these cells of RNase E protomers from, respectively, the ASKA plasmid and the chromosome (since the fold-decrease in expression from chromosomal *rne*$^+$is expected to mirror that from *rne-lac*, with the balance of RNase E polypeptides now being contributed from the non-autoregulated ASKA-encoded gene so that the aggregate number of homo-tetramers in the cell is constant). If one assumes that this proportion is maintained with the ASKA derivatives encoding the mutant polypeptides at 25 μM IPTG, then these cells will be populated with hetero-tetramers in which the mutant to wild-type polypeptide ratio is approximately evenly divided between 2:2 and 3:1 (in addition to, an albeit minor, proportion of the catalytically dead homo-tetrameric 4:0 species).

That there was equivalent induction by 25 μM IPTG from the different ASKA plasmid constructs was tested by comparison of cultures expressing the wild-type and one of the mutant RNase E polypeptides (D303A), and the results from the Western blotting experiment [performed using anti-His antibody, since the proteins encoded by the ASKA plasmid constructs carry N-terminal His-tags (55)], confirmed that this was so (Supplementary Figure S6B). Our data therefore suggest that a full-length RNase E tetramer in which only one (or two) of the polypeptides bears a functional active site possesses the same endonucleolytic activity *in vivo* as another in which the active sites of all four polypeptides are functional, and we refer to this phenomenon as recessive resurrection.

The (full-length) polypeptides with double substitutions R169Q (5′-sensor pocket) and D303A or D346A (active site) also elicited reduction in expression of *rne-lac* with 25μM IPTG supplementation in the chromosomal *rne*$^+$ strains (Supplementary Figure S5D). Even when the polypeptide encoded on the chromosome was RNase E-493Δ, IPTG-induced overexpression of full-length polypeptides bearing the D303A or D346A substitutions (with or without the R169Q substitution as well) was correlated with reduced *rne-lac* expression, indicative of increased *in vivo* RNase E activity under these conditions (Figure 6E).

Given that recessive resurrection was observed with full-length and not the CTH-truncated polypeptides, we asked whether degradosome assembly on the CTH is contributing to the phenomenon. For example, it has been proposed that RNase E-CTH and the degradosome serve as antennae for binding to polysomes to mediate mRNA decay (77), and that stabilization of hypomodified tRNAs in RNase E-ΔCTH derivatives is because of a defect in degradosome assembly (78). We measured *rne-lac* expression in a chromosomal *rne*$^+$ strain in which degradosome assembly was abolished by loss of both RhlB and PNPase proteins, after IPTG-induced overexpression from ASKA plasmids of full-length RNase E without or with D303A or D346A substitutions. Polypeptides with the active site substitutions elicited the same magnitude of reduction in *rne-lac* expression as did wild-type RNase E, indicative of recessive resurrection (Supplementary Figure S5E); at the same time, the extent of reduction (for all three overproduced polypeptides) was less than that in the degradosome-proficient strain (compare Figure 6C and Supplementary Figure S5E), which may reflect the fact that the degradosome proteins are needed for efficient cleavage of at least some RNA substrates by RNase E (79,80).

Measurements of chromosomal *rne*$^+$ expression by RT-qPCR

We then performed RT-qPCR experiments to directly determine changes in expression of the autoregulated chromosomal *rne*$^+$ gene, in derivatives that also carried the ASKA plasmid constructs for RNase E or its variants (IPTG-inducible and not autoregulated). For these measurements, a part of the 5′-UTR of *rne* mRNA was chosen, since this region is encoded only by the native chromosomal *rne*$^+$ gene. The control region was taken from 16S rRNA, as had been done also in an earlier RT-qPCR study to measure *in vivo* RNase E activities (81).

Levels of *rne* 5′-UTR were measured in isogenic derivatives carrying either plasmid vector pCA24N or ASKA constructs for full-length RNase E without or with the active site substitutions D303A or D346A, after growth in medium supplemented with 25 μM IPTG. Compared to the level in the vector-bearing strain, overexpression from the plasmid of wild-type RNase E was associated with a 1.9-fold reduction in mRNA from chromosomal *rne*$^+$, indicative of autoregulation; similar, statistically significant, reductions were also obtained upon overexpression of full-length RNase E with the D303A or D346A substitutions (Figure 7).

DISCUSSION

Several thousand substrates for RNase E exist in bacteria (43,79,82). By examining RNase E variants with C-terminal truncations and active site or 5′-sensor pocket substitutions (by themselves or in different combinations), we identified two new features for this enzyme: intragenic complementation, and the ability of a full-length catalytically dead polypeptide to offer complete functional co-operation *in vivo* when co-expressed with wild-type RNase E (recessive resurrection). On the other hand, active-site substitutions in the CTH-truncated variants were dominant negative.

In several experiments, *rne-lac* expression was used as an inverse proxy for *in vivo* RNase E activity. This notion is so robustly supported by previous studies as to represent the consensus (8,10–12,23,30,45,46,83,84). To this extent, it has been stated that '[*rne-lac*] expression provides a simple means to gauge the level of RNase E activity in the cell' (30), and that '*rne* mRNA serves as a sensor for total cellular RNase E activity' (2). At the same time, we have also validated a key finding by RT-qPCR experiments.

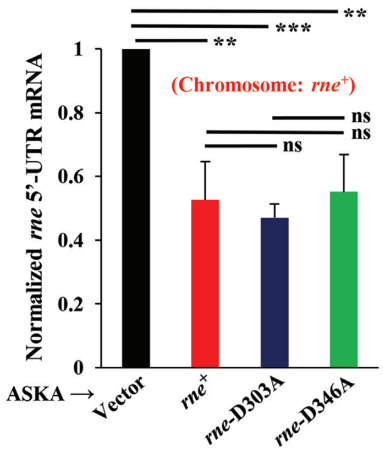

Figure 7. Determination by RT-qPCR of 5′-UTR levels for mRNA expressed from chromosomal *rne*$^+$ locus, after adjustment to 16S rRNA levels in the preparations. Strains (MC4100 transformants with indicated ASKA-derived plasmids) were cultured in LB with Cm and 25 μM IPTG. Values (mean ± SE) are shown after normalization to that in the vector-bearing derivative, taken as 1. Notations adjoining the overlines indicate *P* values for statistical pair-wise comparisons by Student's *t*-test, as follows: **, <0.02; ***, <0.001 and ns, >0.5. Plasmids were: vector, pCA24N; *rne*$^+$, pASKA-*rne*; *rne*-D303A, pHYD5152; and *rne*-D346A, pHYD5151.

Intragenic complementation in RNase E

Intragenic or allelic complementation signifies that two variants encoded by different alleles of a single gene are together able to restore function when neither variant by itself is active (85,86). One possible mechanism is cross-subunit catalysis, but other hypotheses include stabilization of enzyme structure and gene dosage effects.

In RNase E, an R169Q substitution in the 5′-sensor pocket confers inviability when present on a CTH-truncated polypeptide such as 529Δ, 493Δ or 395Δ, while active site substitutions D303A or D346A are lethal in both the full-length and CTH-truncated molecules. Through both *in vivo* and *in vitro* experiments, we demonstrated complementation between pairs of the mutant polypeptides. These data provide support to the cross-subunit model of RNase E catalysis (27). Given the similarity between RNases E and G (31–34,48,49), it is likely that intragenic complementation would occur in the latter.

Substitutions borne on RNase E-395Δ also exhibited intragenic complementation (when the polypeptides were overexpressed), and additional conditions which increase the stringency of RNase E essentiality [such as RNase G deficiency and ppGpp^0 (47,87)] did not affect the outcome. These results, as also the finding that 395Δ is dominant negative, indicate that the 395Δ polypeptides can heterodimerize.

The data from size-exclusion chromatography experiments corroborate the findings of Caruthers *et al.* (48) that 395Δ elutes as a monomer. The polypeptide eluted at larger size in presence of RNA, suggesting that it dimerizes upon RNA binding. By a similar approach, we showed also that dimerization of RNase E-493Δ is promoted by RNA binding.

A cartoon model in Figure 8 depicts the concepts of RNA-facilitated oligomerization, cross-subunit catalysis, and intragenic complementation with respect to the 395Δ truncation in RNase E. It is likely that electrostatic and other non-covalent interactions between the interfacing large domains of two 395Δ polypeptides also contribute to dimer stabilization.

Mechanistic role of the CTH for recessive resurrection in RNase E

The fact that active-site substitutions are subject to recessive resurrection when borne on full-length RNase E, but are not so on CTH-truncated derivatives such as 493Δ, suggests that the CTH is involved in mediating the phenomenon. Although the CTH is dispensable for viability, it does contribute to enzyme function *in vivo* (7,9,18,19,34,44–47,77,83,88–90; and this study). The properties attributed to the CTH include degradosome assembly (14–19,22), membrane localization (20,21,23), RNA binding (18,19,24), and association with other proteins and sRNAs (4,25,26). We have shown that the capacity to augment RNase E activity by overexpression of the mutant polypeptides is preserved (to the same extent as equivalent overexpression of wild-type RNase E) in strains lacking both PNPase and RhlB, suggesting that degradosome assembly is not necessary for recessive resurrection. However, any one or more of the other functions attributed to the CTH may be responsible for the phenomenon.

We propose that the CTH participates in a rate-determining step of RNase E function that precedes RNA 5′-sensing and endonucleolytic cleavage by the NTH. One possibility is that it traps and channels RNA to the NTH, for subsequent steps of enzyme action. Thus, a relatively slow rate of cleavage on account of only one or two active protomers being present in the tetramer may have little or no effect on overall enzyme activity. It is only in absence of the CTH that the number of active subunits in an oligomer (tetramer or dimer) becomes important in determining the catalysis rate, and hence it is that active site mutations elicit dominant negative phenotypes when they are on CTH-truncated peptides. Jain *et al.* (30) had also previously proposed a role for the CTH in RNA binding and presentation to the NTH.

The CTH of RNase E is less conserved than is the NTH (91). In *Caulobacter crescentus*, as in *E. coli*, the CTH is unstructured and binds RNA; however, unlike in *E. coli*, the degradosome assembled on its CTH forms liquid-liquid phase-separated condensates (92). In actinobacteria including *Streptomyces coelicolor* and *Mycobacterium tuberculosis*, RNase E does appear to assemble a degradosome but the non-catalytic regions are shuffled with respect to the catalytic domain (93–95).

Recessive resurrection as a novel genetic phenomenon

In simple genetic parlance, loss of function mutations are recessive (to wild-type) while gain of function mutations are dominant. Dominant negative mutations represent a special category, in that they are loss of function mutations that act by a subunit poisoning mechanism within oligomeric complexes to confer a dominant phenotype (75,76).

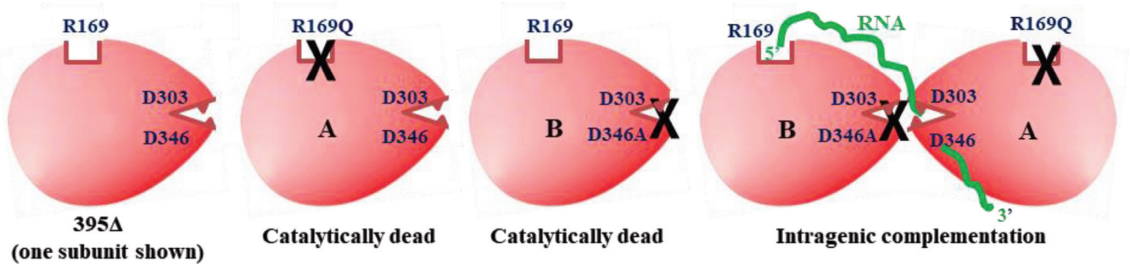

Figure 8. Cartoon to depict intragenic complementation by RNA-facilitated oligomerization and cross-subunit catalysis between a pair of RNase E-395Δ polypeptides, one (**A**) with 5′-sensor (R169Q) and the other (**B**) with active-site (D346A) disruption.

Recessive resurrection refers to loss of function mutations that become indistinguishable from the wild-type allele in an heterozygous situation. The mutant polypeptides in hetero-oligomeric complexes would thus appear to have recovered full activity. A common mechanistic assumption underlying dominant negativity and recessive resurrection is that of random assembly of subunits into oligomers from amongst the pool of co-expressed polypeptides.

Interestingly, RNase III of *E. coli* is an oligomeric endoribonuclease (dimer) with an N-terminal catalytic domain and a C-terminal domain that binds RNA but is dispensable for catalytic activity (96,97). An RNase III heterodimer of wild-type and catalytically inactive subunits was reported to retain full activity (98), which if true would constitute another example of recessive resurrection. However, another group has claimed that substrate turnover rate for the hetero-dimer is one-half that for the wild-type homodimer (99). Furthermore, unlike in RNase E, the active site substitution of RNase III is dominant negative (100).

It is likely that examples of recessive resurrection occur in other systems. One approach to identify them in diploid organisms may be to focus on genes that are known to display haploinsufficiency phenotypes (101–103), and then to identify missense mutations in them which (i) lead to a loss of function in the homozygote, and yet (ii) create no haploinsufficiency defect in the heterozygous individual.

SUPPLEMENTARY DATA

Supplementary Data are available at NAR Online.

ACKNOWLEDGEMENTS

We thank Krishna Leela, T.S. Shaffiqu and members of the Ranjan Sen lab for assistance with experiments; and K. Anupama and COE team members for advice and discussions.

FUNDING

Centre of Excellence (COE) project for Microbial Biology – Phase 2 from the Department of Biotechnology (DBT), Govt of India; DBT Junior and Senior Research Fellowships (N.A.); J.C. Bose National Fellowship and INSA Senior Scientist award (to J.G.).
Conflict of interest statement. None declared.

REFERENCES

1. Arraiano,C.M., Andrade,J.M., Domingues,S., Guinote,I.B., Malecki,M., Matos,R.G., Moreira,R.N., Pobre,V., Reis,F.P., Saramago,M. *et al.* (2010) The critical role of RNA processing and degradation in the control of gene expression. *FEMS Microbiol. Rev.*, **34**, 883–923.
2. Mackie,G.A. (2013) RNase E: at the interface of bacterial RNA processing and decay. *Nat. Rev. Microbiol.*, **11**, 45–57.
3. Hui,M.P., Foley,P.L. and Belasco,J.G. (2014) Messenger RNA degradation in bacterial cells. *Annu. Rev. Genet.*, **48**, 537–559.
4. Aït-Bara,S. and Carpousis,A.J. (2015) RNA degradosomes in bacteria and chloroplasts: classification, distribution and evolution of RNase E homologs. *Mol. Microbiol.*, **97**, 1021–1035.
5. Mohanty,B.K. and Kushner,S.R. (2018) Enzymes involved in posttranscriptional RNA metabolism in Gram-negative bacteria. *Microbiol. Spectr.*, **6**, RWR-0011–2017.
6. Bandyra,K.J. and Luisi,B.F. (2018) RNase E and the high-Fidelity orchestration of RNA metabolism. *Microbiol. Spectr.*, **6**, RWR-0008–2017.
7. Mudd,E.A. and Higgins,C.F. (1993) *Escherichia coli* endoribonuclease RNase E: autoregulation of expression and site-specific cleavage of mRNA. *Mol. Microbiol.*, **9**, 557–568.
8. Jain,C. and Belasco,J.G. (1995) RNase E autoregulates its synthesis by controlling the degradation rate of its own mRNA in *Escherichia coli*: unusual sensitivity of the rne transcript to RNase E activity. *Genes Dev.*, **9**, 84–96.
9. Ow,M.C., Liu,Q. and Kushner,S.R. (2000) Analysis of mRNA decay and rRNA processing in *Escherichia coli* in the absence of RNase E-based degradosome assembly. *Mol. Microbiol.*, **38**, 854–866.
10. Sousa,S., Marchand,I. and Dreyfus,M. (2001) Autoregulation allows *Escherichia coli* RNase E to adjust continuously its synthesis to that of its substrates. *Mol. Microbiol.*, **42**, 867–878.
11. Jain,C., Deana,A. and Belasco,J.G. (2002) Consequences of RNase E scarcity in *Escherichia coli*. *Mol. Microbiol.*, **43**, 1053–1064.
12. Diwa,A., Bricker,A.L., Jain,C. and Belasco,J.G. (2000) An evolutionarily conserved RNA stem-loop functions as a sensor that directs feedback regulation of RNase E gene expression. *Genes Dev.*, **14**, 1249–1260.
13. Schuck,A., Diwa,A. and Belasco,J.G. (2009) RNase E autoregulates its synthesis in *Escherichia coli* by binding directly to a stem-loop in the *rne* 5′ untranslated region. *Mol. Microbiol.*, **72**, 470–478.
14. Carpousis,A.J., Van Houwe,G., Ehretsmann,C. and Krisch,H.M. (1994) Copurification of *E. coli* RNAase E and PNPase: evidence for a specific association between two enzymes important in RNA processing and degradation. *Cell*, **76**, 889–900.
15. Py,B., Higgins,C.F., Krisch,H.M. and Carpousis,A.J. (1996) A DEAD-box RNA helicase in the *Escherichia coli* RNA degradosome. *Nature*, **381**, 169–172.
16. Miczak,A., Kaberdin,V.R., Wei,C.L. and Lin-Chao,S. (1996) Proteins associated with RNase E in a multicomponent ribonucleolytic complex. *Proc. Natl. Acad. Sci. U.S.A.*, **93**, 3865–3869.
17. Vanzo,N.F., Li,Y.S., Py,B., Blum,E., Higgins,C.F., Raynal,L.C., Krisch,H.M. and Carpousis,A.J. (1998) Ribonuclease E organizes the protein interactions in the *Escherichia coli* RNA degradosome. *Genes Dev.*, **12**, 2770–2781.

18. Callaghan,A.J., Aurikko,J.P., Ilag,L.L., Grossmann,G.J., Chandran,V., Kühnel,K., Poljak,L., Carpousis,A.J., Robinson,C. V., Symmons,M.F. *et al.* (2004) Studies of the RNA degradosome-organizing domain of the *Escherichia coli* ribonuclease RNase E. *J. Mol. Biol.*, **340**, 965–979.
19. Worrall,J.A.R., Górna,M., Crump,N.T., Phillips,L.G., Tuck,A.C., Price,A.J., Bavro,V.N. and Luisi,B.F. (2008) Reconstitution and analysis of the multienzyme *Escherichia coli* RNA degradosome. *J. Mol. Biol.*, **382**, 870–883.
20. Khemici,V., Poljak,L., Luisi,B.F. and Carpousis,A.J. (2008) The RNase E of *Escherichia coli* is a membrane-binding protein. *Mol. Microbiol.*, **70**, 799–813.
21. Murashko,O.N., Kaberdin,V.R. and Lin-Chao,S. (2012) Membrane binding of *Escherichia coli* RNase E catalytic domain stabilizes protein structure and increases RNA substrate affinity. *Proc. Natl. Acad. Sci. U.S.A.*, **109**, 7019–7024.
22. Strahl,H., Turlan,C., Khalid,S., Bond,P.J., Kebalo,J.-M., Peyron,P., Poljak,L., Bouvier,M., Hamoen,L., Luisi,B.F. *et al.* (2015) Membrane Recognition and Dynamics of the RNA Degradosome. *PLos Genet.*, **11**, e1004961.
23. Hadjeras,L., Poljak,L., Bouvier,M., Morin-Ogier,Q., Canal,I., Cocaign-Bousquet,M., Girbal,L. and Carpousis,A.J. (2019) Detachment of the RNA degradosome from the inner membrane of *Escherichia coli* results in a global slowdown of mRNA degradation, proteolysis of RNase E and increased turnover of ribosome-free transcripts. *Mol. Microbiol.*, **111**, 1715–1731.
24. Kaberdin,V.R., Walsh,A.P., Jakobsen,T., McDowall,K.J. and von Gabain,A. (2000) Enhanced cleavage of RNA mediated by an interaction between substrates and the arginine-rich domain of *E. coli* ribonuclease E. *J. Mol. Biol.*, **301**, 257–264.
25. Morita,T., Maki,K. and Aiba,H. (2005) RNase E-based ribonucleoprotein complexes: mechanical basis of mRNA destabilization mediated by bacterial noncoding RNAs. *Genes Dev.*, **19**, 2176–2186.
26. Bruce,H.A., Du,D., Matak-Vinkovic,D., Bandyra,K.J., Broadhurst,R.W., Martin,E., Sobott,F., Shkumatov,A.V. and Luisi,B.F. (2018) Analysis of the natively unstructured RNA/protein-recognition core in the *Escherichia coli* RNA degradosome and its interactions with regulatory RNA/Hfq complexes. *Nucleic Acids Res.*, **46**, 387–402.
27. Callaghan,A.J., Marcaida,M.J., Stead,J.A, McDowall,K.J., Scott,W.G. and Luisi,B.F. (2005) Structure of *Escherichia coli* RNase E catalytic domain and implications for RNA turnover. *Nature*, **437**, 1187–1191.
28. Koslover,D.J., Callaghan,A.J., Marcaida,M.J., Garman,E.F., Martick,M., Scott,W.G. and Luisi,B.F. (2008) The crystal structure of the Escherichia coli RNase E apoprotein and a mechanism for RNA degradation. *Structure*, **16**, 1238–1244.
29. Callaghan,A.J., Redko,Y., Murphy,L.M., Grossmann,J.G., Yates,D., Garman,E., Ilag,L.L., Robinson,C. V., Symmons,M.F., McDowall,K.J. *et al.* (2005) 'Zn-Link': A metal-sharing interface that organizes the quaternary structure and catalytic site of the endoribonuclease, RNase E. *Biochemistry*, **44**, 4667–4675.
30. Briegel,K.J., Baker,A. and Jain,C. (2006) Identification and analysis of *Escherichia coli* ribonuclease E dominant-negative mutants. *Genetics*, **172**, 7–15.
31. Jiang,X. and Belasco,J.G. (2004) Catalytic activation of multimeric RNase E and RNase G by 5′-monophosphorylated RNA. *Proc. Natl. Acad. Sci. U.S.A.*, **101**, 9211–9216.
32. Mackie,G.A. (1998) Ribonuclease E is a 5′-end-dependent endonuclease. *Nature*, **395**, 720–724.
33. Tock,M.R., Walsh,A.P., Carroll,G. and McDowall,K.J. (2000) The CafA protein required for the 5′-maturation of 16 S rRNA is a 5′-end-dependent ribonuclease that has context-dependent broad sequence specificity. *J. Biol. Chem.*, **275**, 8726–8732.
34. Garrey,S.M., Blech,M., Riffell,J.L., Hankins,J.S., Stickney,L.M., Diver,M., Hsu,Y.-H.R., Kunanithy,V. and Mackie,G.A. (2009) Substrate binding and active site residues in RNases E and G. *J. Biol. Chem.*, **284**, 31843–31850.
35. Coburn,G.A. and Mackie,G.A. (1999) Degradation of mRNA in *Escherichia coli*: an old problem with some new twists. *Prog. Nucleic Acid Res. Mol. Biol.*, **62**, 55–108.
36. Bandyra,K.J., Wandzik,J.M. and Luisi,B.F. (2018) Substrate recognition and autoinhibition in the central ribonuclease RNase E. *Mol. Cell*, **72**, 275–285.
37. Deana,A., Celesnik,H. and Belasco,J.G. (2008) The bacterial enzyme RppH triggers messenger RNA degradation by 5′ pyrophosphate removal. *Nature*, **451**, 355–358.
38. Luciano,D.J., Vasilyev,N., Richards,J., Serganov,A. and Belasco,J.G. (2017) A novel RNA phosphorylation state enables 5′ end-dependent degradation in *Escherichia coli*. *Mol. Cell*, **67**, 44–54.
39. Richards,J. and Belasco,J.G. (2019) Obstacles to scanning by RNase E govern bacterial mRNA lifetimes by hindering access to distal cleavage sites. *Mol. Cell*, **74**, 284–295.
40. Baker,K.E. and Mackie,G.A. (2003) Ectopic RNase E sites promote bypass of 5′-end-dependent mRNA decay in *Escherichia coli*. *Mol. Microbiol.*, **47**, 75–88.
41. Kime,L., Jourdan,S.S., Stead,J.A., Hidalgo-Sastre,A. and McDowall,K.J. (2010) Rapid cleavage of RNA by RNase E in the absence of 5′ monophosphate stimulation. *Mol. Microbiol.*, **76**, 590–604.
42. Kime,L., Clarke,J.E., Romero,A.D., Grasby,J.A. and McDowall,K.J. (2014) Adjacent single-stranded regions mediate processing of tRNA precursors by RNase E direct entry. *Nucleic Acids Res.*, **42**, 4577–4589.
43. Clarke,J.E., Kime,L., Romero,A.D. and McDowall,K.J. (2014) Direct entry by RNase E is a major pathway for the degradation and processing of RNA in *Escherichia coli*. *Nucleic Acids Res.*, **42**, 11733–11751.
44. Joyce,S.A. and Dreyfus,M. (1998) In the absence of translation, RNase E can bypass 5′ mRNA stabilizers in *Escherichia coli*. *J. Mol. Biol.*, **282**, 241–254.
45. Anupama,K., Leela,J.K. and Gowrishankar,J. (2011) Two pathways for RNase E action in *Escherichia coli in vivo* and bypass of its essentiality in mutants defective for Rho-dependent transcription termination. *Mol. Microbiol.*, **82**, 1330–1348.
46. Garrey,S.M. and Mackie,G.A. (2011) Roles of the 5′-phosphate sensor domain in RNase E. *Mol. Microbiol.*, **80**, 1613–1624.
47. Himabindu,P. and Anupama,K. (2017) Decreased expression of stable RNA can alleviate the lethality associated with RNase E deficiency in *Escherichia coli*. *J. Bacteriol.*, **199**, e00724-16.
48. Caruthers,J.M., Feng,Y., McKay,D.B. and Cohen,S.N. (2006) Retention of core catalytic functions by a conserved minimal ribonuclease E peptide that lacks the domain required for tetramer formation. *J. Biol. Chem.*, **281**, 27046–27051.
49. Jourdan,S.S. and McDowall,K.J. (2008) Sensing of 5′ monophosphate by *Escherichia coli* RNase G can significantly enhance association with RNA and stimulate the decay of functional mRNA transcripts *in vivo*. *Mol. Microbiol.*, **67**, 102–115.
50. Baek,Y.M., Jang,K.-J., Lee,H., Yoon,S., Baek,A., Lee,K. and Kim,D.-E. (2019) The bacterial endoribonuclease RNase E can cleave RNA in the absence of the RNA chaperone Hfq. *J. Biol. Chem.*, **294**, 16465–16478.
51. Nilsson,R.-P., Gabain,A. von and Kaberdin,V.R. (2002) In-gel analysis of site-specific RNases. *BioTechniques*, **33**, 272–276.
52. Miller,J.H. (1992) *A Short Course in Bacterial Genetics : A Laboratory Manual and Handbook for Escherichia coli and Related Bacteria*. Cold Spring Harbor Lab Press, NY.
53. Baba,T., Ara,T., Hasegawa,M., Takai,Y., Okumura,Y., Baba,M., Datsenko,K.A., Tomita,M., Wanner,B.L. and Mori,H. (2006) Construction of *Escherichia coli* K-12 in-frame, single-gene knockout mutants: the Keio collection. *Mol. Syst. Biol.*, **2**, 2006.0008.
54. Vimala,A. and Harinarayanan,R. (2016) Transketolase activity modulates glycerol-3-phosphate levels in *Escherichia coli*. *Mol. Microbiol.*, **100**, 263–277.
55. Kitagawa,M., Ara,T., Arifuzzaman,M., Ioka-Nakamichi,T., Inamoto,E., Toyonaga,H. and Mori,H. (2005) Complete set of ORF clones of *Escherichia coli* ASKA library (*A* complete *S*et of *E. coli K*-12 ORF *A*rchive): unique resources for biological research. *DNA Res.*, **12**, 291–299.
56. Wang,R.F. and Kushner,S.R. (1991) Construction of versatile low-copy-number vectors for cloning, sequencing and gene expression in *Escherichia coli*. *Gene*, **100**, 195–199.

57. Nazir,A. and Harinarayanan,R. (2016) Inactivation of cell division protein FtsZ by SulA makes Lon indispensable for the viability of a ppGpp^0 strain of *Escherichia coli*. *J. Bacteriol.*, **198**, 688–700.
58. Datsenko,K.A. and Wanner,B.L. (2000) One-step inactivation of chromosomal genes in *Escherichia coli* K-12 using PCR products. *Proc. Natl. Acad. Sci. U.S.A.*, **97**, 6640–6645.
59. Gowrishankar,J. (1985) Identification of osmoresponsive genes in Escherichia coli: evidence for participation of potassium and proline transport systems in osmoregulation. *J. Bacteriol.*, **164**, 434–445.
60. Sambrook,J. and Russell,D. (2001) *Molecular Cloning: A Laboratory Manual*. 3rd edn. Cold Spring Harbor Lab Press, NY.
61. Court,D.L., Swaminathan,S., Yu,D., Wilson,H., Baker,T., Bubunenko,M., Sawitzke,J. and Sharan,S.K. (2003) Mini-lambda: a tractable system for chromosome and BAC engineering. *Gene*, **315**, 63–69.
62. Reddy,M. and Gowrishankar,J. (2000) Characterization of the *uup* locus and its role in transposon excisions and tandem repeat deletions in *Escherichia coli*. *J. Bacteriol.*, **182**, 1978–1986.
63. Bustin,S.A., Benes,V., Garson,J.A., Hellemans,J., Huggett,J., Kubista,M., Mueller,R., Nolan,T., Pfaffl,M.W., Shipley,G.L. *et al.* (2009) The MIQE guidelines: minimum information for publication of quantitative real-time PCR experiments. *Clin. Chem.*, **55**, 611–622.
64. Guenin,S., Mauriat,M., Pelloux,J., Van Wuytswinkel,O., Bellini,C. and Gutierrez,L. (2009) Normalization of qRT-PCR data: the necessity of adopting a systematic, experimental conditions-specific, validation of references. *J. Exp. Bot.*, **60**, 487–493.
65. Studier,F.W., Rosenberg,A.H., Dunn,J.J. and Dubendorff,J.W. (1990) Use of T7 RNA polymerase to direct expression of cloned genes. *Methods Enzymol.*, **185**, 60–89.
66. Valabhoju,V., Agrawal,S. and Sen,R. (2016) Molecular basis of NusG-mediated regulation of Rho-dependent transcription termination in bacteria. *J. Biol. Chem.*, **291**, 22386–22403.
67. Shin,E., Go,H., Yeom,J.H., Won,M., Bae,J., Seung,H.H., Han,K., Lee,Y., Ha,N.C., Moore,C.J. *et al.* (2008) Identification of amino acid residues in the catalytic domain of RNase E essential for survival of *Escherichia coli*: functional analysis of DNase I subdomain. *Genetics*, **179**, 1871–1879.
68. Leela,J.K., Syeda,A.H., Anupama,K. and Gowrishankar,J. (2013) Rho-dependent transcription termination is essential to prevent excessive genome-wide R-loops in *Escherichia coli*. *Proc. Natl. Acad. Sci. U.S.A.*, **110**, 258–263.
69. Raghunathan,N., Kapshikar,R.M., Leela,J.K., Mallikarjun,J., Bouloc,P. and Gowrishankar,J. (2018) Genome-wide relationship between R-loop formation and antisense transcription in *Escherichia coli*. *Nucleic Acids Res.*, **46**, 3400–3411.
70. Raghunathan,N., Goswami,S., Leela,J.K., Pandiyan,A. and Gowrishankar,J. (2019) A new role for *Escherichia coli* Dam DNA methylase in prevention of aberrant chromosomal replication. *Nucleic Acids Res.*, **47**, 5698–5711.
71. Gowrishankar,J. (2015) End of the beginning: elongation and termination features of alternative modes of chromosomal replication initiation in bacteria. *PLoS Genet.*, **11**, e1004909.
72. Callaghan,A.J., Grossmann,J.G., Redko,Y.U., Ilag,L.L., Moncrieffe,M.C., Symmons,M.F., Robinson,C. V., McDowall,K.J. and Luisi,B.F. (2003) Quaternary structure and catalytic activity of the *Escherichia coli* ribonuclease E amino-terminal catalytic domain. *Biochemistry*, **42**, 13848–13855.
73. Redko,Y., Tock,M.R., Adams,C.J., Kaberdin,V.R., Grasby,J.A. and McDowall,K.J. (2003) Determination of the catalytic parameters of the N-terminal half of *Escherichia coli* ribonuclease E and the identification of critical functional groups in RNA substrates. *J. Biol. Chem.*, **278**, 44001–44008.
74. Grossmann,J.G., Callaghan,A.J., Marcaida,M.J., Luisi,B.F., Alcock,F.H., Tokatlidis,K., Moulin,M., Haertlein,M. and Timmins,P. (2008) Complementing structural information of modular proteins with small angle neutron scattering and contrast variation. *Eur. Biophys. J.*, **37**, 603–611.
75. Herskowitz,I. (1987) Functional inactivation of genes by dominant negative mutations. *Nature*, **329**, 219–222.
76. Veitia,R.A. (2007) Exploring the molecular etiology of dominant-negative mutations. *Plant Cell*, **19**, 3843–3851.
77. Tsai,Y.-C., Du,D., Domínguez-Malfavón,L., Dimastrogiovanni,D., Cross,J., Callaghan,A.J., García-Mena,J. and Luisi,B.F. (2012) Recognition of the 70S ribosome and polysome by the RNA degradosome in *Escherichia coli*. *Nucleic Acids Res.*, **40**, 10417–10431.
78. Kimura,S. and Waldor,M.K. (2019) The RNA degradosome promotes tRNA quality control through clearance of hypomodified tRNA. *Proc. Natl. Acad. Sci. U.S.A.*, **116**, 1394–1403.
79. Bernstein,J.A., Khodursky,A.B., Lin,P.-H., Lin-Chao,S. and Cohen,S.N. (2002) Global analysis of mRNA decay and abundance in *Escherichia coli* at single-gene resolution using two-color fluorescent DNA microarrays. *Proc. Natl. Acad. Sci. U.S.A.*, **99**, 9697–9702.
80. Khemici,V., Poljak,L., Toesca,I. and Carpousis,A.J. (2005) Evidence in vivo that the DEAD-box RNA helicase RhlB facilitates the degradation of ribosome-free mRNA by RNase E. *Proc. Natl. Acad. Sci. U.S.A.*, **102**, 6913–6918.
81. Luciano,D.J., Hui,M.P., Deana,A., Foley,P.L., Belasco,K.J. and Belasco,J.G. (2012) Differential control of the rate of 5′-end-dependent mRNA degradation in *Escherichia coli*. *J. Bacteriol.*, **194**, 6233–6239.
82. Chao,Y., Li,L., Girodat,D., Förstner,K.U., Said,N., Corcoran,C., Śmiga,M., Papenfort,K., Reinhardt,R., Wieden,H.-J. *et al.* (2017) In vivo cleavage map illuminates the central role of RNase E in coding and non-coding RNA pathways. *Mol. Cell*, **65**, 39–51.
83. Leroy,A., Vanzo,N.F., Sousa,S., Dreyfus,M. and Carpousis,A.J. (2002) Function in *Escherichia coli* of the non-catalytic part of RNase E: role in the degradation of ribosome-free mRNA. *Mol. Microbiol.*, **45**, 1231–1243.
84. Lee,K., Zhan,X., Gao,J., Qiu,J., Feng,Y., Meganathan,R., Cohen,S.N. and Georgiou,G. (2003) RraA. a protein inhibitor of RNase E activity that globally modulates RNA abundance in E. coli. *Cell*, **114**, 623–634.
85. McGavin,S. (1968) Interallelic complementation and allostery. *J. Mol. Biol.*, **37**, 239–242.
86. Juers,D.H., Matthews,B.W. and Huber,R.E. (2012) *LacZ* β-galactosidase: structure and function of an enzyme of historical and molecular biological importance. *Protein Sci.*, **21**, 1792–1807.
87. Tamura,M., Kers,J.A. and Cohen,S.N. (2012) Second-site suppression of RNase E essentiality by mutation of the *deaD* RNA helicase in *Escherichia coli*. *J. Bacteriol.*, **194**, 1919–1926.
88. Kido,M., Yamanaka,K., Mitani,T., Niki,H., Ogura,T. and Hiraga,S. (1996) RNase E polypeptides lacking a carboxyl-terminal half suppress a *mukB* mutation in *Escherichia coli*. *J. Bacteriol.*, **178**, 3917–3925.
89. Lopez,P.J., Marchand,I., Joyce,S.A. and Dreyfus,M. (1999) The C-terminal half of RNase E, which organizes the *Escherichia coli* degradosome, participates in mRNA degradation but not rRNA processing *in vivo*. *Mol. Microbiol.*, **33**, 188–199.
90. Jiang,X., Diwa,A. and Belasco,J.G. (2000) Regions of RNase E important for 5′-end-dependent RNA cleavage and autoregulated synthesis. *J.Bacteriol.*, **182**, 2468–2475.
91. Kaberdin,V.R., Miczak,A., Jakobsen,J.S., Lin-Chao,S., McDowall,K.J. and von Gabain,A. (1998) The endoribonucleolytic N-terminal half of *Escherichia coli* RNase E is evolutionarily conserved in *Synechocystis sp*. and other bacteria but not the C-terminal half, which is sufficient for degradosome assembly. *Proc. Natl. Acad. Sci. U.S.A.*, **95**, 11637–11642.
92. Al-Husini,N., Tomares,D.T., Bitar,O., Childers,W.S. and Schrader,J.M. (2018) α-Proteobacterial RNA degradosomes assemble liquid-liquid phase-separated RNP bodies. *Mol. Cell*, **71**, 1027–1039.
93. Lee,K. and Cohen,S.N. (2003) A *Streptomyces coelicolor* functional orthologue of *Escherichia coli* RNase E shows shuffling of catalytic and PNPase-binding domains. *Mol. Microbiol.*, **48**, 349–360.
94. Zeller,M.-E., Csanadi,A., Miczak,A., Rose,T., Bizebard,T. and Kaberdin,V.R. (2007) Quaternary structure and biochemical properties of mycobacterial RNase E/G. *Biochem. J.*, **403**, 207–215.
95. Płociński,P., Macios,M., Houghton,J., Niemiec,E., Płocińska,R., Brzostek,A., Słomka,M., Dziadek,J., Young,D. and Dziembowski,A. (2019) Proteomic and transcriptomic experiments reveal an essential role of RNA degradosome complexes in shaping the transcriptome of *Mycobacterium tuberculosis*. *Nucleic Acids Res.*, **47**, 5892–5905.
96. Sun,W., Jun,E. and Nicholson,A.W. (2001) Intrinsic double-stranded-RNA processing activity of *Escherichia coli*

ribonuclease III lacking the dsRNA-binding domain. *Biochemistry*, **40**, 14976–14984.
97. Nicholson,A.W. (2014) Ribonuclease III mechanisms of double-stranded RNA cleavage. *Wiley Interdiscip. Rev. RNA*, **5**, 31–48.
98. Conrad,C., Schmitt,J.G., Evguenieva-Hackenberg,E. and Klug,G. (2002) One functional subunit is sufficient for catalytic activity and substrate specificity of *Escherichia coli* endoribonuclease III artificial heterodimers. *FEBS Lett.*, **518**, 93–96.
99. Meng,W. and Nicholson,A.W. (2008) Heterodimer-based analysis of subunit and domain contributions to double-stranded RNA processing by *Escherichia coli* RNase III *in vitro*. *Biochem. J.*, **410**, 39–48.
100. Dasgupta,S., Fernandez,L., Kameyama,L., Inada,T., Nakamura,Y., Pappas,A. and Court,D.L. (1998) Genetic uncoupling of the dsRNA-binding and RNA cleavage activities of the *Escherichia coli* endoribonuclease RNase III – the effect of dsRNA binding on gene expression. *Mol. Microbiol.*, **28**, 629–640.
101. Deutschbauer,A.M., Jaramillo,D.F., Proctor,M., Kumm,J., Hillenmeyer,M.E., Davis,R.W., Nislow,C. and Giaever,G. (2005) Mechanisms of haploinsufficiency revealed by genome-wide profiling in yeast. *Genetics*, **169**, 1915–1925.
102. Dang,V.T., Kassahn,K.S., Marcos,A.E. and Ragan,M.A. (2008) Identification of human haploinsufficient genes and their genomic proximity to segmental duplications. *Eur. J. Hum. Genet.*, **16**, 1350–1357.
103. Huang,N., Lee,I., Marcotte,E.M. and Hurles,M.E. (2010) Characterising and predicting haploinsufficiency in the human genome. *PLoS Genet.*, **6**, e1001154.